

Analysis of Flow of Viscous Fluids by the Finite-Element Method

J. TINSLEY ODEN* AND L. CARTER WELLFORD JR.†

University of Alabama, Huntsville, Ala.

General finite-element models of compressible and incompressible fluid flow are derived. These involve local approximations of the velocity field, the density, and the temperature for compressible fluids and the velocity, temperature, and pressure for incompressible fluids. Theories of local solenoidal approximations and mixed finite-element models for compressible flow are derived. A number of computational schemes are developed for the numerical solution of both transient and steady nonuniform flow problems involving incompressible fluids. Numerical results obtained from several test problems are given. It is shown that the finite element method has great potential for use in flow problems, and represents a powerful new tool for the analysis of viscous flows.

Introduction

THE present paper is concerned with the application of the concept of finite elements to the formulation and solution of a wide range of problems in fluid dynamics. The method is sufficiently general to treat a variety of unsteady and nonlinear flow phenomena in irregular domains. An intrinsic feature of finite-element approximations is that a mathematical model is generated by patching together a number of purely "local" approximations of the phenomena under consideration. This aspect of the method effectively frees the analyst from traditional difficulties associated with irregular geometries, multi-connected domains, and mixed boundary conditions. Moreover, applications are firmly rooted in the physics of the problem at hand and preliminary studies indicate that, for a given order of accuracy, the resulting equations are better conditioned than those obtained by, say, finite difference approximations of the governing differential equations.¹

Certain of the underlying ideas of the finite element method were discussed in 1943 by Courant.² However, the formal presentation of the method is generally attributed to the 1956 paper of Turner et al.³ While the method has found wide application in solid and structural mechanics,⁴ its application to flow problems has come only in rather recent times. Early uses of the method were always associated with variational statements of the problem under consideration, so that it is natural that steady, potential flow problems were the first to be solved using finite elements. We mention, in this regard, the works of Zienkiewicz, Mayer, and Cheung⁵ on seepage through porous media and Martin⁶ on potential flow problems. Finite element models of unsteady compressible and incompressible flow problems were obtained by Oden.⁷⁻¹⁰ Applications of finite element methods to a number of important problems in fluid mechanics have been reported in recent years; among them, we mention the work of Thompson, Mack, and Lin¹¹ on steady incompressible flow and Tong,¹² Fujino,¹³ Argyris et al.,¹⁴⁻¹⁶ Reddi,¹⁷ Baker,¹⁸ and Herting, Joseph, Kuusinen, and MacNeal¹⁹ on various special incompressible flow problems. The recent book of Zienkiewicz⁴ can be consulted for additional references.

In the present investigation, we extend the finite element method to general three-dimensional problems of heat conduction and flow of compressible and incompressible fluids, wherein no restriction is placed on the constitution or equation of state

of the fluid under consideration. Effectively, we develop finite element analogues of the equations of continuity, linear momentum, and energy of arbitrary fluids. The models are obtained from local approximations of the density, velocity, and temperature fields in each element and represent generalizations of those proposed earlier.^{7,9}

In addition, we treat the problem of fluids characterized by equations of state in which the thermodynamic pressure is not given explicitly as a function of the density, temperature, and velocity gradients. There we develop mixed finite-element models by approximating locally the mean stress (or thermodynamic pressure) in each element. We obtain a general model in which the equation of state is satisfied in an average sense over each element. We then consider the special but important case of viscous incompressible fluids, with emphasis on isotropic Newtonian fluids with constant viscosities. There we address ourselves to certain problems connected with imposing the continuity equation (incompressibility condition) in the discrete model and to special boundary conditions. A notion of solenoidal finite element fields is introduced. We then describe computational schemes for the solutions of the equations governing the model for uniform steady flow, nonuniform steady flow, and unsteady flow of viscous fluids. Numerical results obtained from applications to a number of representative example problems are presented.

Finite Element Models of Fluid Flow

To fix ideas, consider the motion of a continuous medium through some closed region R of three-dimensional euclidean space. We establish in R a fixed inertial frame of reference defined by orthonormal basis vectors i_i ($i = 1, 2, 3$). The spatial coordinates of a place P in R are denoted x_i and the components of velocity of the medium at P at time t are denoted $v_i(x_1, x_2, x_3, t) \equiv v_i(x, t)$. The density and the absolute temperature at place P at time t are denoted $\rho(x, t)$ and $\theta(x, t)$, respectively. If T_0 denotes a uniform temperature at some reference time t_0 , we may use as an alternate temperature measure the temperature change $T(x, t) = \theta(x, t) - T_0$.

To construct a finite element model of the fluid, we replace R by a domain \bar{R} consisting of a finite number E of subdomains r_e , so that $R \approx \bar{R} = \cup_{e=1}^E r_e$. The subregions r_e are the finite elements; they are generally of simple geometric shapes and are designed so as to represent a good approximation of R when appropriately connected together. The geometry of each finite element r_e is characterized by a finite number N_e of nodal places (the number may vary from element to element) and the nodes of a typical element e are defined by the spatial coordinates $x_{i(e)}^N$; $N = 1, 2, \dots, N_e$; $i = 1, 2, 3$; $e = 1, 2, \dots, E$. The global finite element model \bar{R} is obtained by connecting the E discrete elements at appropriate nodal points by means of simple incidence

Received December 1, 1971; revision received May 24, 1972. Support of this work by the U.S. Air Force Office of Scientific Research under Contract F44620-69-C-0124 is gratefully acknowledged.

Index categories: Viscous Nonboundary-Layer Flows; Boundary Layers and Convective Heat Transfer-Laminar.

* Professor and Chairman, Department of Engineering Mechanics, Member AIAA.

† Graduate Student, and Engineer, Teledyne Brown Engineering.

mappings which merely identify the desired correspondence between local and global nodal labels. These mappings are described elsewhere²⁰ and need not be discussed here. The important feature of the model is its local character; that is, the behavior of the medium can be idealized locally in a typical element independent of the behavior in other elements in the model and independent of its ultimate location in the model. The final global model is then obtained by routinely connecting elements together through mappings which depend only upon the topology of the model.

Following guidelines provided by the notion of determinism,²² we shall take as our fundamental dependent variables, the velocity, mass density, and temperature change as obvious measures of these primitive characteristics. Therefore, consider a typical finite element r_e with N_e nodes isolated from the global model \bar{R} . Let $\mathbf{v}(\mathbf{x}, t)$, $\rho(\mathbf{x}, t)$, and $T(\mathbf{x}, t)$ denote global approximations of the velocity, density, and temperature change to be determined at $\mathbf{x} \in \bar{R}$ at time t , and let $\mathbf{v}_{(e)}$, $\rho_{(e)}$, and $T_{(e)}$ denote their restrictions to element r_e . Then finite-element approximations of these restrictions are constructed which are of the form

$$\mathbf{v}_{(e)} = \psi_N^{(e)}(\mathbf{x})\mathbf{v}_{(e)N}^N(t) \tag{1a}$$

$$\rho_{(e)} = \phi_N^{(e)}(\mathbf{x})\rho_{(e)N}^N(t) \tag{1b}$$

$$T_{(e)} = \chi_N^{(e)}(\mathbf{x})T_{(e)N}^N(t) \tag{1c}$$

Here and henceforth the repeated nodal indices are summed from 1 to N_e ; $\mathbf{v}_{(e)N}^N(t)$, $\rho_{(e)N}^N(t)$, and $T_{(e)N}^N(t)$ are the values of the velocity, density, and relative temperature at node N of element r_e at time t ; i.e.

$$\mathbf{v}_{(e)N}^N(t) \equiv \mathbf{v}_{(e)}(\mathbf{x}_{(e)N}^N, t) \tag{2}$$

etc. The functions $\psi_N^{(e)}(\mathbf{x})$, $\phi_N^{(e)}(\mathbf{x})$, and $\chi_N^{(e)}(\mathbf{x})$ are local interpolation functions defined so as to have the properties

$$\psi_N^{(e)}(\mathbf{x}) = 0, \quad \mathbf{x} \notin r_e; \quad \psi_N^{(e)}(\mathbf{x}^M) = \delta_{NM}; \quad \sum_{N=1}^{N_e} \psi_N^{(e)}(\mathbf{x}) = 1 \tag{3}$$

Notice that Eq. (1) implies that different forms of the interpolation functions may be used to approximate different local fields over the same finite element. In certain cases (some of which are to be discussed later), this may require that certain of the functions vanish at certain nodal points or that indices N in each member of Eq. (1) may have different ranges. Note also that "higher order" local representations can be obtained by also specifying values of derivatives of \mathbf{v} , ρ , and T at the nodes.

We must also remark that, in the case of incompressible fluids, our formulation requires that, instead of the density $\rho_{(e)}(\mathbf{x}, t)$ we approximate the pressure field $p(\mathbf{x}, t)$ over \bar{R} . Thus, if $p_{(e)}(\mathbf{x}, t)$ is the restriction of $p(\mathbf{x}, t)$ to r_e , we assume

$$p_{(e)} = \mu_N^{(e)}(\mathbf{x})p_{(e)N}^N(t) \tag{4}$$

The interpolation functions $\mu_N^{(e)}(\mathbf{x})$ also obey Eq. (3).

Mechanics of a Finite Element

Kinematics

With the local velocity field given by Eq. (1a), all relevant kinematical quantities associated with the motion of the element are determined by the nodal velocities $\mathbf{v}_{(e)N}^N(t)$. For example, the components of local acceleration are

$$a_i = Dv_i/Dt = \partial v_i/\partial t + v_{i,m}v_m = \psi_N \dot{v}_i^N + \psi_{N,m} \psi_M v_i^M v_m^M \tag{5}$$

where $\dot{v}_i^N = dv_i^N(t)/dt$, commas denote partial differentiation with respect to the spatial coordinates (i.e. $\psi_{N,m} \equiv \partial \psi_N(\mathbf{x})/\partial x_m$), the repeated indices are, again, summed over their admissible ranges ($i, m = 1, 2, 3$; $M, N = 1, 2, \dots, N_e$), and the element identification label (e) has been dropped for simplicity. Likewise, the models of the rate-of-deformation tensor d_{ij} and the spin tensor w_{ij} are given by

$$d_{ij} = \frac{1}{2}(\psi_{N,i} v_j^N + \psi_{N,j} v_i^N) \quad w_{ij} = \frac{1}{2}(\psi_{N,i} v_j^N - \psi_{N,j} v_i^N) \tag{6}$$

and the local vorticity field ω_i is $\omega_i = \varepsilon_{ijk} \psi_{N,k} v_j^N$, where ε_{ijk} is the permutation symbol. Local approximations of various other kinematical quantities can be calculated in a similar manner.

Momentum Equations for a Finite Element

The equations governing the motion of a typical finite element can be obtained by constructing a Galerkin integral of Cauchy's first law of motion over the element and by using the velocity interpolation functions $\psi_N(\mathbf{x})$ as weight functions in this integral. If this approach is taken, linear momentum is balanced in an average sense over the element. The arbitrariness of the choice of $\psi_N(\mathbf{x})$ as weight functions, however, is removed if an alternate but equivalent approach based on energy balances is employed.⁹

The behavior of the medium must be consistent with the principle of conservation of energy:

$$D/Dt(\kappa + U) = \Omega + Q \tag{7}$$

where κ is the kinetic energy, U is the internal energy, Ω is the mechanical power, and Q is the heat:

$$\begin{aligned} \kappa &= \frac{1}{2} \int_v \rho v_j v_j dv & U &= \int_v \rho \varepsilon dv \\ \Omega &= \int_v \rho F_j v_j dv + \int_A S_j v_j dA & Q &= \int_v \rho h dv + \int_A q_j n_j dA \end{aligned} \tag{8}$$

In Eq. (8) ε is the internal energy density, F_j are the components of the body force vector per unit mass, S_j are components of the surface tractions, h is the heat per unit mass supplied from internal sources, q_j are the components of heat flux, and n_j is the normal to the boundary surface. Noting that the material derivative of the kinetic energy for element e is

$$D\kappa/Dt = \int_{v_e} \rho v_j a_j dv$$

and introducing Eq. (5) and (1a), we obtain

$$(D/Dt)\kappa = [c_{MNL} \rho^M \dot{v}_k^L + d_{MNLP}^m \rho^M v_m^L v_k^P] v_k^N \tag{9}$$

where

$$c_{MNL} = \int_{v_e} \varphi_M \psi_N \psi_L dv, \quad d_{MNLP}^m = \int_{v_e} \varphi_M \psi_N \psi_L \psi_{P,m} dv \tag{10}$$

and $M, N, L, P = 1, \dots, N_e$. The first quantity in parenthesis represents the local inertial force at node N in the k th direction, and the second term in the parenthesis represents the convective inertial force at node N in the k th direction.

Since the local form of the energy balance is

$$\rho(D\varepsilon/Dt) = \rho \dot{\varepsilon} + \rho v_i \varepsilon_i = T_{ik} v_{k,i} + q_{k,k} + \rho h \tag{11}$$

wherein T_{ik} is the Cauchy stress tensor, the material derivative of the internal energy for the element can be written as

$$DU_e/Dt = v_k^N \int_{v_e} T_{ik} \psi_{N,i} dv + Q_e \tag{12}$$

where $Q_e = \int_{v_e} (q_{k,k} + \rho h) dv$ is the heat of the element. For an element of fluid of volume v_e and surface area A_e , the power of external forces is

$$\Omega = \left[\int_{A_e} T_{ik} n_i \psi_N dA + C_{RNk} \rho^R \right] v_k^N \tag{13}$$

where

$$C_{RNk} = \int_{v_e} \varphi_R F_k \psi_N dv$$

The first and second quantities in the parenthesis represent the force at node N in the k th direction due to the surface stress distribution and the force at node N in the k th direction due to the body force, respectively. If we define the generalized force p_{Nk} according to

$$p_{Nk} = \int_{A_e} S_k \psi_N dA + C_{RNk} \rho^R \tag{14}$$

then the generalized forces develop the same amount of mechanical power as the external forces in the continuum element, and

$$\Omega_e = p_{Nk} v_k^N$$

Finally, introducing Eqs. (9), (12), and Ω_e into (7), we obtain an energy equation for a typical finite element e . Then, making the

argument that this result must hold for arbitrary values of the nodal velocity v_k^N , we obtain as the general equations of motion (momentum) for a compressible fluid element:

$$c_{MNL} \rho^M v_k^L + d_{MNL}^m \rho^M v_m^L v_k^P + \int_{v_e} T_{ik} \psi_{N,i} dv - p_{Nk} = 0 \quad (15)$$

The constitutive equation for stress in terms of the approximate velocity and pressure expressions must be introduced to complete this equation.

The Continuity Equation for an Element

The local form of the continuity equation is

$$\dot{\rho} + (\rho v_k)_k = 0 \quad (16)$$

where $\dot{\rho} \equiv \partial \rho / \partial t$. Introducing Eqs. (1a) and (1b) into (16) yields at point \mathbf{x} the residual

$$r_e(\mathbf{x}) = \varphi_N(\mathbf{x}) \dot{\rho}^N + (\varphi_N(\mathbf{x}) \psi_R(\mathbf{x}))_{,k} \rho^N v_k^R \quad (17)$$

We can guarantee that the residual vanishes in an average sense over the element by requiring that it be orthogonal (with respect to the inner product $\langle f, g \rangle = \int_{v_e} f g dv$) to the subspace spanned by the functions $\varphi_M(\mathbf{x})$. Then $\langle r_e, \varphi_M \rangle = \int_{v_e} r_e \varphi_M dv = 0$, and we obtain the finite element model of the continuity equation:

$$a_{MN} \dot{\rho}^N + b_{MNR}^k \rho^N v_k^R = 0 \quad (18)$$

Here $M, N, R = 1, 2, \dots, N_e$ and a_{MN} and b_{MNR}^k denote the local arrays

$$a_{MN} = \int_{v_e} \varphi_M \varphi_N dv, \quad b_{MNR}^k = \int_{v_e} \varphi_M (\varphi_N \psi_R)_{,k} dv \quad (19)$$

Energy Equation for an Element

By introducing Eq. (1a) into the local form of the first law, Eq. (11), we obtain the residual

$$\hat{r}_e = \varphi_R \rho^R \dot{\varepsilon} + \varphi_R \rho^R \psi_N v_i^N \varepsilon_i - T_{ik} \psi_{N,i} v_k^N - q_{k,k} - \varphi_R \rho^R h \quad (20)$$

Here it is understood that ε , T_{ik} , and q_k are functions of the local fields defined in Eqs. (1). As before, we require that the residual be orthogonal to the subspace spanned by the $\chi_M(\mathbf{x})$ functions:

$$\langle \hat{r}_e, \chi_M \rangle = \int_{v_e} \hat{r}_e \chi_M dv = 0 \quad (21)$$

Introduction of Eq. (20) into Eq. (21) gives the general finite element analogue of the energy equation:

$$\int_{v_e} \varphi_R \dot{\varepsilon} \chi_M dv \rho^R + \int_{v_e} \varphi_R \psi_N \varepsilon_i \chi_M dv \rho^R v_i^N = \int_{v_e} T_{ik} \psi_{N,i} \chi_M dv v_k^N - \int_{v_e} \chi_M q_k dv + \int_{A_e} \chi_M q_k n_k dA + \int_{v_e} \varphi_R h \chi_M dv \rho^R \quad (22)$$

In order to obtain a useable expression for the energy constitutive equations must be introduced for stress T_{ik} , internal energy density ε , heat flux q_k , and heat produced by internal sources h .

We remark that an alternate equation of heat conduction can be obtained for the element by rewriting Eq. (11) in terms of the entropy density $\eta(\mathbf{x}, t)$ and the internal dissipation $\sigma(\mathbf{x}, t) = \rho \theta \dot{\eta} - q_{k,k} - \rho h$. For these choices of variables, a procedure similar to that used to obtain Eq. (15) yields the general equation of heat conduction for an element,

$$\rho^M \int_{v_e} \varphi_M \chi_N (T_0 + \chi_p T^p) \left(\frac{\partial \eta}{\partial t} + \psi_{R,m} v_m^R \eta_m \right) dv + \int_{v_e} q_i \chi_{N,i} dv = q_N + \sigma_N \quad (23)$$

Here q_N and σ_N are the generalized normal heat flux and the generalized internal dissipation at node N

$$q_N = \int_{v_e} h \chi_N dv + \int_{A_e} q_i n_i \chi_N dA \quad \sigma_N = \int_{v_e} \sigma \chi_N dv \quad (24)$$

Again, the procedure used to derive Eq. (23) is equivalent to Galerkin's method and specific forms can be obtained when constitutive equations for η and q_i are furnished.

Constitutive Equations, Equations of State, and Mixed Models

Equations (15), (18), and (22) [or Eq. (23)] describe the general equations of motion, continuity, and energy (or heat conduction) of a typical element in a finite-element model of an arbitrary fluid. To apply these equations to a specific fluid, it is necessary to eliminate ε , T_{ij} , q_k , and possibly η by introducing appropriate constitutive equations which uniquely define these functions in terms of $v_{(e)}$, $\rho_{(e)}$ and $T_{(e)}$. This is the customary procedure in finite-element formulations.

In the case of compressible fluids, however, the mean stress or the thermodynamic pressure often appears implicitly in the equation of state of the fluid, and it may be impossible or impractical to obtain T_{ij} explicitly as a function of ρ , $v_{i,j}$, and T . In such cases, we propose that a "mixed" finite-element formulation be used, the basis of which is now to be described.

Consider a class of fluids described by constitutive equations for the stress tensor of the form

$$T_{ij} = \delta_{ij} \pi(\rho, d_{rs}, T) + \hat{T}_{ij}(\rho, d_{rs}, T) \quad (25)$$

Here π is the so called thermodynamic pressure and \hat{T}_{ij} is the dissipative stress. Generally \hat{T}_{ij} is given explicitly as a function of ρ , d_{rs} , and T (e.g., for a class of Stokesian fluids, $\hat{T}_{ij} = 2\mu d_{ij}$, μ being the viscosity); however, π is defined implicitly by an equation of state:

$$F(\pi, d_{ij}, \rho, T) = 0 \quad (26)$$

Assuming that we cannot (or do not choose to) eliminate π from Eq. (25) by use of Eq. (26) we propose a mixed finite-element model in which the restriction $\pi_e(\mathbf{x}, t)$ of π to element r_e is assumed to be of the form

$$\pi_e = \beta_N(\mathbf{x}) \pi^N(t) \quad (27)$$

The interpolation functions $\beta_N(\mathbf{x})$ have properties similar to Eq. (3). Introducing Eq. (1) and (27) into (26), we obtain a residual r_e^* . Then, the condition $\langle r_e^*, \beta_N \rangle = 0$ leads to the N_e local equations

$$\int_{v_e} \beta_N F(\beta_N \pi^N, \psi_{N,i} v_i^N, \varphi_N \rho^N, \chi_N T^N) dv = 0 \quad (28)$$

Equation (28) represents the finite-element analogue of the equation of state, Eq. (26), and insure that it is satisfied in a weighted average sense over each finite element. Introduction of Eq. (27) into (25) and incorporation of the result into Eqs. (15), (18), and (22) [or Eq. (23)] (along with constitutive equations for q_k , ε , and h as functions of ρ , T , and $v_{i,j}$) yields a complete system of equations in the nodal values of velocity, density, temperature, and thermodynamic pressure.

Incompressible Fluids

We shall now consider purely mechanical behavior of incompressible fluids. Here two principal considerations are involved: 1) all motions are volume-preserving and 2) the stress tensor is not completely determined by the motion. The first condition reveals that ρ is now a known constant and the continuity equation reduces to the incompressibility condition

$$\text{div } \mathbf{v} = d_{ii} = v_{i,i} = 0 \quad (29)$$

The second consideration suggests that $\pi = -p$, p being the hydrodynamic pressure, and that the local pressure of Eq. (4) should be selected as an unknown in place of ρ .

Considering now ρ to be known and following essentially the same procedure used to obtain Eq. (15), we obtain for the general equation of motion of incompressible elements

$$m_{MN} v_k^N + n_{MNP}^m v_m^N v_k^P + h_{MNk} p^N + \int_{v_e} \hat{T}_{ik} \psi_{M,i} dv = p_{Mk} \quad (30)$$

where m_{MN} and n_{MNP}^m are the mass and convected mass "matrices" respectively, h_{MNk} is an array of pressure coefficients, and p_{Mk} are the components of the generalized force defined by Eq. (14)

$$m_{MN} = \int_{v_e} \rho \psi_M \psi_N dv \quad n_{MNP}^m = \int_{v_e} \rho \psi_M \psi_N \psi_{P,m} dv$$

$$h_{MNk} = - \int_{v_e} \mu \psi_M \psi_{N,k} dv \quad (31)$$

The derivation of the incompressibility constraint can best be cast in physical terms: Observe that the work done by the pressure p due to a change in volume dv is clearly $p_e \nabla \cdot v dv = p_e v_{i,i}^{(e)} dv$. But p_e can perform no work since for incompressible flow $\nabla \cdot v$ is zero. It follows that for a finite element of an incompressible fluid,

$$\int_{v_e} p_e v_{i,i}^{(e)} dv = \int_{v_e} \mu_M \psi_{N,i} dv p^M v_i^N = 0$$

This relation must hold for arbitrary p^M ; thus the finite element model for the incompressibility condition is,

$$r_{MN}^i v_i^N = 0; \quad r_{MN}^i = \int_{v_e} \mu_M \psi_{N,i} dv \quad (32)$$

We note that the energy equation, Eq. (22), is also modified slightly for incompressible elements due to the fact that $\varphi_N \rho^N$ is now replaced by its presumed known value and \hat{T}_{ik} depends on p^N . These alterations are straightforward and need not be described here.

Incompressible Newtonian Fluids

The special case of an incompressible Newtonian flow with constant viscosity is of special interest because a number of classical solutions to various flow problems are available for comparisons. Of course, since the viscosity is constant, the energy equation is uncoupled from the momentum and continuity equations and they may be solved separately. For the Newtonian fluid the dissipative stress tensor is simply $\hat{T}_{ik} = 2\mu d_{ik}$, μ being the viscosity. Thus, for the finite element, $\hat{T}_{ik} = \mu(\psi_{N,k} v_i^N + \psi_{N,i} v_k^N)$ and Eq. (30) reduces to

$$m_{MN} v_k^N + n_{MNP}^m v_k^P + h_{MNk} p^N + z_{MN} v_k^N + w_{MN}^{ik} v_i^N = p_{Mk} \quad (33)$$

where

$$z_{MN} = \int_{v_e} \mu \psi_{M,i} \psi_{N,i} dv \quad \text{and} \quad w_{MN}^{ik} = \int_{v_e} \mu \psi_{M,i} \psi_{N,k} dv \quad (34)$$

To these equations we add the incompressibility conditions, Eqs. (32), to form a determinate set.

Boundary Conditions

If either the total stress or the velocity is specified at the boundary of a finite element model, no particular difficulties are encountered; the prescribed stress is introduced directly into Eq. (14) to obtain consistent generalized nodal forces, and the nodal velocities are prescribed to satisfy the "nonslip" boundary condition at a fixed or moving wall or the specified velocity distribution on other surfaces. In this respect, the procedure differs very little from that employed in the finite element analysis of solids. However, in fluids, specification of the stress at a boundary may not uniquely determine the pressure; moreover, the boundary conditions may represent constraints on the pressure or its gradient rather than the total stress. In these situations, it may be necessary to develop special analogues of the boundary conditions.

Consider, for example, the generalized force of Eq. (14) in the case of an incompressible fluid. Ignoring the body force term temporarily, we observe that

$$p_{Nk} = \int_{A_e} T_{ik} n_i \psi_N dA = \int_{A_e} (-p \delta_{ik} + \hat{T}_{ik}) n_i \psi_N dA$$

or

$$p_{Nk} = \hat{p}_{Nk} + \int_{A_e} \hat{T}_{ik} n_i \psi_N dA; \quad \hat{p}_{Nk} = - \int_{A_e} p n_k \psi_N dA \quad (35)$$

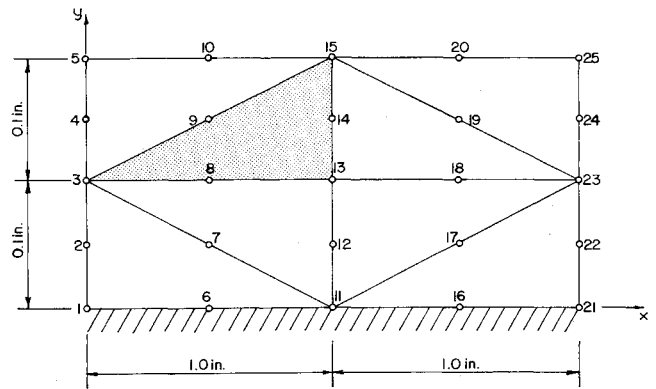


Fig. 1 Finite-element model for the calculation of Couette flow.

The quantity \hat{p}_{Nk} is the generalized nodal force due to prescribed pressures p on the boundary.

Similar procedures can be used for various other special boundary conditions. For example, it is not uncommon to use as a condition at the impermeable boundary with zero velocity the specification of the pressure gradient as a function of the body force and the acceleration (i.e., $p_{,n} = \rho F_n - \rho a_n$ where the subscript n refers to the normal direction to the wall). This boundary condition can either be applied by retaining the momentum equation at the nodes in contact with the fixed wall or by applying a discrete version at the nodes in contact with the wall. The first method, which is followed herein, satisfies the boundary condition in an average sense over the boundary elements. The second method satisfies the boundary condition exactly at the wall nodes.

The first method is obtained directly from the discrete momentum equation, Eq. (33), by setting $v_k^N = 0$ (for boundary nodes N) and $\hat{T}_{ik} = 0$, since \hat{T}_{ik} depends only on v_k^N there. Then

$$m_{MN} v_k^N + h_{MNk} p^N = f_{Mk} - \int_{A_e} p n_k \psi_M dA$$

where $f_{Mk} = \int_{v_e} \rho F_k \psi_M dv$ is the generalized force at node M due to the body forces F_k . Transforming the surface integral via the Green-Gauss theorem and collecting terms, we arrive at the discrete analogue of the pressure-gradient boundary condition,

$$g_{MNk} p^N = f_{Mk} - m_{MN} v_k^N \quad (36)$$

wherein $g_{MNk} = \int_{v_e} \psi_M \mu_{N,k} dv$.

In the second method, a discrete version of this type of boundary condition can be obtained for element e by merely introducing Eq. (4) into the local statement of the boundary condition and evaluating the result at the coordinates of each of the wall nodes. While this leads to a cruder approximation, it is nevertheless much easier to apply in actual calculations.

Solenoidal Approximations

The pressure term $h_{MNk} p^N$ can be eliminated from the discrete momentum equation Eq. (33) by constructing solenoidal finite-element approximations of the local velocity. We accomplish this by introducing so called "bubble functions" $\alpha_i(\mathbf{x})$ which vanish on the boundaries of each element and which satisfy (at least approximately) the condition

$$\alpha_{i,i} = -\psi_{N,i}(\mathbf{x}) v_i^N \quad (37)$$

Any particular integral of Eq. (37) vanishing on ∂R_e is of the form

$$\alpha_i(\mathbf{x}) = \alpha_i^j(\mathbf{x}) v_j^N \quad (38)$$

The incompressibility condition, Eq. (29) is now satisfied locally by local velocity approximations of the form

$$v_i^e(\mathbf{x}, t) = \bar{\psi}_{N,i}^j(\mathbf{x}) v_j^N; \quad \bar{\psi}_{N,i}^j = \delta_i^j \psi_N(\mathbf{x}) + \alpha_i^j(\mathbf{x}) \quad (39)$$

The remaining terms in Eq. (33) are altered accordingly.

The use of local solenoidal velocity fields makes it possible to eliminate the hydrodynamic pressure term from the discrete

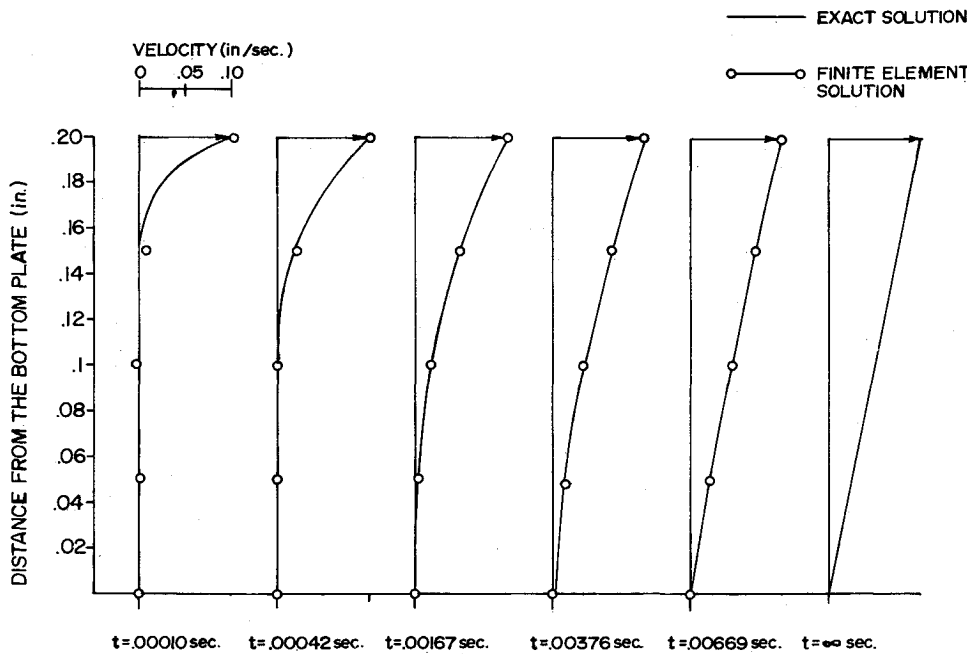


Fig. 2 Velocity profile at various time points for transient Couette flow.

momentum equations, Eqs. (33). Thus the momentum equations can be solved directly for the local velocity fields. Then the pressure calculation can be performed independently based on the computed velocity field.

The pressure must satisfy Poisson's equation.

$$p_{,ii} = \bar{T}_{ij,ji}(\mathbf{x}, v_i^N) + \rho F_{i,i} - \rho a_{i,i} \quad (40)$$

where $\bar{T}_{ij}(\mathbf{x}, v_i^N)$ is the dissipative part of the stress tensor. This can be verified by taking the divergence of the local momentum equation.²² The solution of this equation by means of finite elements is very well documented.⁴

Numerical Techniques

In order to obtain a preliminary estimate of the applicability of the foregoing theory, we consider a series of classical problems in two-dimensional incompressible Newtonian flow. Several numerical techniques are developed herein to handle problems

of this type. With minor changes, these techniques could be applied to three-dimensional incompressible flow problems or, in general, to any isothermal incompressible viscous fluid.

Consider the solution of the system of equations consisting of the momentum equation, Eq. (33), and the continuity equation, Eq. (32). Three cases can be analyzed based on the properties of the flow: steady uniform flow; steady nonuniform flow; and transient or unsteady flow. The models developed earlier lead to systems of linear algebraic equations in the first case, nonlinear algebraic equations in the second, and nonlinear differential equations in the third.

Steady, Uniform Linear Flow

For the steady flow problem, the term $m_{MN}^N v_k^N$ and the convective term $n_{MNP}^m v_m^N v_k^P$ in Eq. (33) vanish and the linearized momentum equation takes the form

$$h_{MNk}^N + z_{MN}^N v_k^N + w_{MN}^{ik} v_i^N = p_{Mk} \quad (41)$$

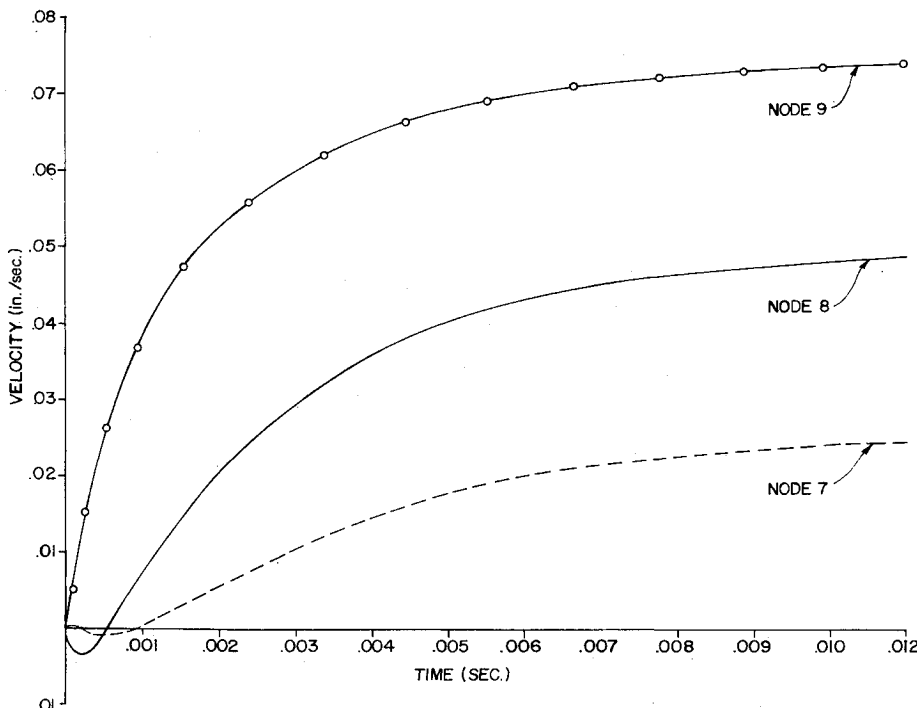


Fig. 3 Time history of the x velocity components at nodes 7, 8, and 9 for transient Couette flow.

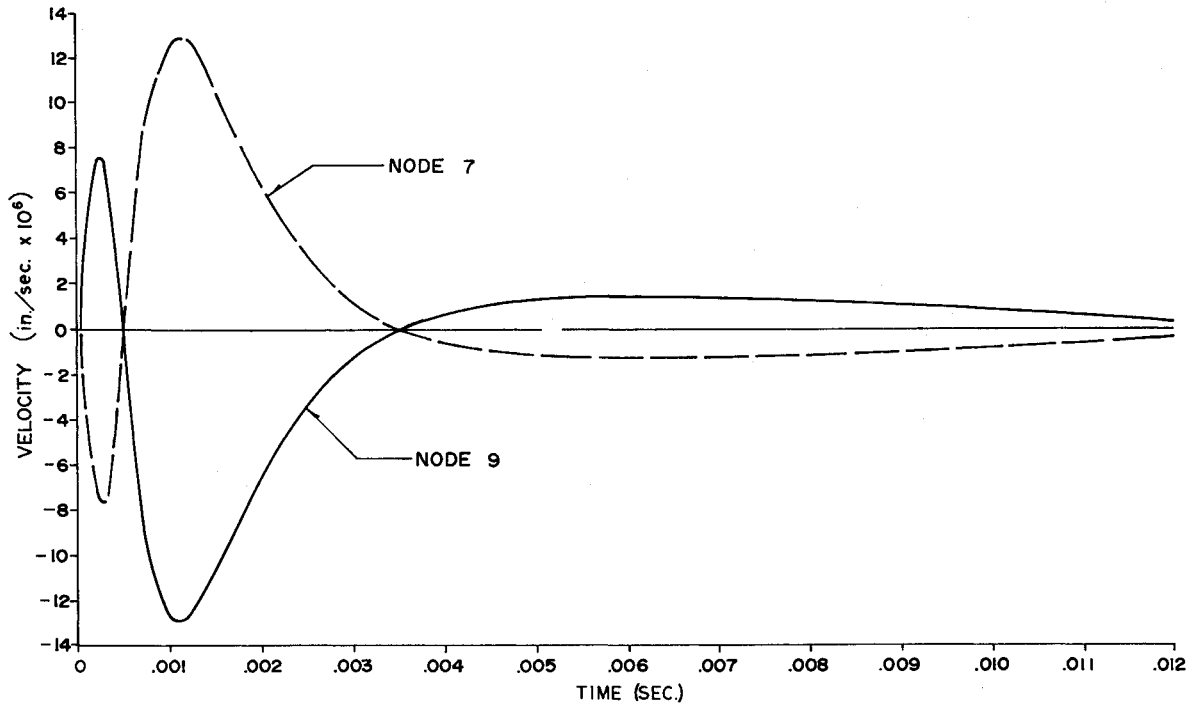


Fig. 4 Time history of y velocity component at nodes 7 and 9 for transient Couette flow.

Equations (41) and (32) represent, for the two-dimensional case, a set of $3N_e$ algebraic equations in $3N_e$ unknowns. Taking note of the fact that $r_{MN}^i = -h_{NMi}$, we can express these equations in matrix form as

$$\begin{bmatrix} z_{MN} + w_{MN}^{11} & w_{MN}^{12} & h_{MN1} \\ w_{MN}^{21} & z_{MN} + w_{MN}^{22} & h_{MN2} \\ -r_{NM}^1 & -r_{NM}^2 & 0 \end{bmatrix} \begin{bmatrix} [v_1^N] \\ [v_2^N] \\ [p^N] \end{bmatrix} = \begin{bmatrix} [p_{M1}] \\ [p_{M2}] \\ [0] \end{bmatrix} \quad (42)$$

The coefficient matrix is square and symmetric. In addition, upon assembling the elements, the global form is sparse and banded. Boundary conditions must be applied in accordance with the previous discussion and the resulting set of equations can be solved for the velocity and pressure variables using standard Gauss-elimination codes.

Steady, Nonuniform Flow—The Method of Incremental Densities

The momentum equation for steady nonlinear flow can be obtained from Eq. (33) by setting the local inertial term $m_{MN} v_k^N$ equal to zero and using the fact that $n_{MNP}^m = \rho r_{MNP}^m$, where

$r_{MNP}^m = \int_{v_e} \psi_M \psi_N \psi_{P,m} dv$. Thus, we obtain the system of nonlinear equations

$$\rho v_{MNP}^m v_m^N v_k^P + h_{MNP}^m v_k^N + z_{MN} v_k^N + w_{MN}^{ik} v_i^N = p_{Mk} \quad (43)$$

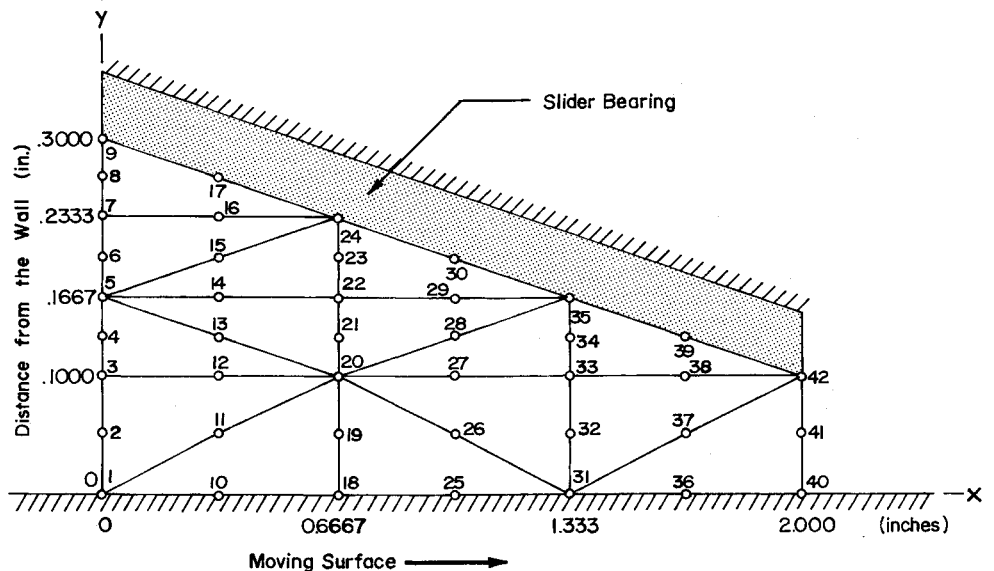
A natural choice of a technique for solving Eqs. (43) is the incremental loading method used in nonlinear structural mechanics.²⁰ This conclusion is based on the observation that if density ρ is assumed to be the loading parameter, when the density equals zero the set of equations reduces to the stationary linear system, Eq. (42), which can be solved using methods described above.

This solution process can be described concisely in vector notation. Suppose that the collection of momentum equations and continuity equations are expressed in vector form as

$$f(v, \rho) = 0 \quad (44)$$

where v is the vector of unknown velocity components and pressures and ρ is the density parameter. Let v be a solution vector corresponding to a particular value of density ρ , and let $v + \delta v$ be a solution vector corresponding to the value of density

Fig. 5 Finite-element model of steady flow of a lubricant through a plane slider bearing.



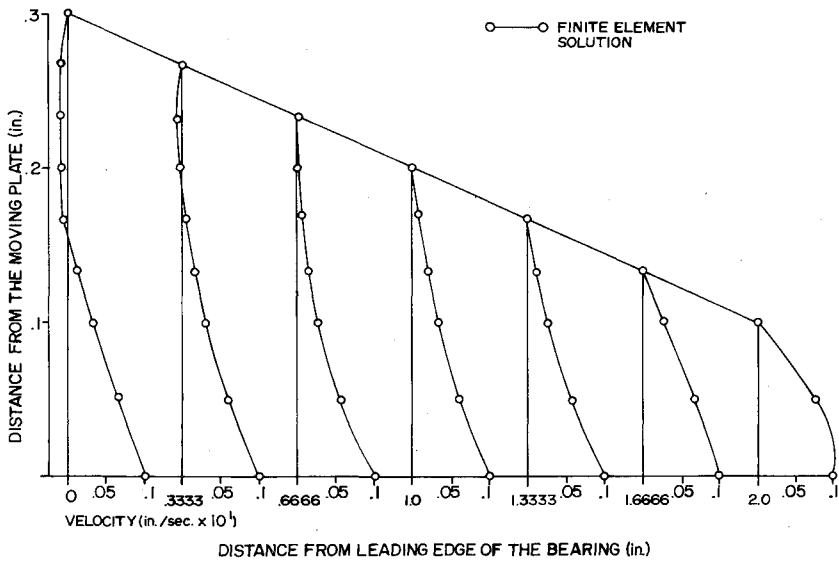


Fig. 6 x velocity component for the lubrication problem.

$\rho + \delta\rho$. Then $\mathbf{f}(\mathbf{v} + \delta\mathbf{v}, \rho + \delta\rho)$ also vanishes. A Taylor's series expansion can be introduced in the neighborhood of \mathbf{v} if $\mathbf{f}(\mathbf{v}, \rho)$ is continuously differentiable at \mathbf{v} . Thus

$\mathbf{f}(\mathbf{v} + \delta\mathbf{v}, \rho + \delta\rho) = \mathbf{f}(\mathbf{v}, \rho) + \mathbf{B}\delta\mathbf{v} + \mathbf{C}\delta\rho + \text{higher order terms}$
 where \mathbf{B} is an $N \times N$ matrix and \mathbf{C} is an $N \times 1$ vector: $B_{ij}(\mathbf{v}, \rho) = \partial f_i(\mathbf{v}, \rho) / \partial v_j$; $C_i(\mathbf{v}, \rho) = \partial f_i(\mathbf{v}, \rho) / \partial \rho$ $i, j = 1, \dots, N$. Thus, within terms of first order, we have the linear system $\mathbf{B}\delta\mathbf{v} = -\mathbf{C}\delta\rho$. Given the initial value of the solution vector \mathbf{v}_0 and the initial value of the density $\rho_0 = 0$, the series expansion forms the basis of an iterative scheme for which the $n + 1$ TH iterate is given by

$$\mathbf{v}_{n+1} = \mathbf{v}_n - \mathbf{B}^{-1}(\mathbf{v}_n, \rho_n)\mathbf{C}(\mathbf{v}_n, \rho_n)\delta\rho_{n+1}; \quad \rho_{n+1} = \sum_{i=1}^{n+1} \delta\rho_i \quad (45)$$

This procedure amounts to a piecewise linearization and the number of iterations should be determined by accuracy requirements.

Unsteady Flow

We shall present results in the next section in which the solution of the system of nonlinear differential equations, Eqs. (32) and (33), were integrated numerically using a self-correcting 4th order Runge-Kutta technique. To outline the essential features, consider first Eq. (33) rewritten in the form

$$\dot{v}_k^L = m_{LM}^{-1} F_{Mk} \quad (46)$$

where

$$F_{Mk} = -n_{MNP}^m v_m^N v_k^L - h_{Mnk} P^N - z_{MN} v_k^N - w_{MN}^{ik} v_i^N + p_{Mk} \quad (47)$$

and m_{LM}^{-1} is the inverse of the mass matrix m_{LM} . The first derivative of the pressure variable can be formulated in similar fashion. We differentiate Eq. (46) with respect to time to obtain

$$\dot{v}_k^L = -m_{LM}^{-1} h_{Mnk} \dot{P}^N + m_{LM}^{-1} H_{Mk}$$

where

$$H_{Mk} = -n_{MNP}^m v_m^N v_k^L - z_{MN} v_k^N - w_{MN}^{ik} v_i^N + p_{Mk}$$

By differentiating Eq. (32) twice we observe that $r_{UL}^k \dot{v}_k^L = 0$; consequently

$$x_{UN} P^N = y_U; \quad x_{UN} = r_{UL}^k m_{LM}^{-1} h_{Mnk}; \quad y_U = r_{UL}^k m_{LM}^{-1} H_{Mk} \quad (48)$$

If h_{VU} is the inverse of x_{UN} , we obtain the explicit expression for the derivative of the pressure variable

$$\dot{P}^N = h_{VU} y_U \quad (49)$$

Equations (46) and (49) are now of the form $\dot{\mathbf{x}} = \mathbf{F}(\mathbf{x}, t)$, which can be directly integrated by standard Runge-Kutta schemes.

Some Numerical Results

We shall now cite representative numerical results obtained by applying the theory and methods presented earlier to specific problems in two-dimensional flow of incompressible Newtonian fluids. For demonstration purposes, we shall employ six-node triangular elements of the type shown in Fig. 1, for which the local velocity and pressure fields are given by the quadratic polynomials

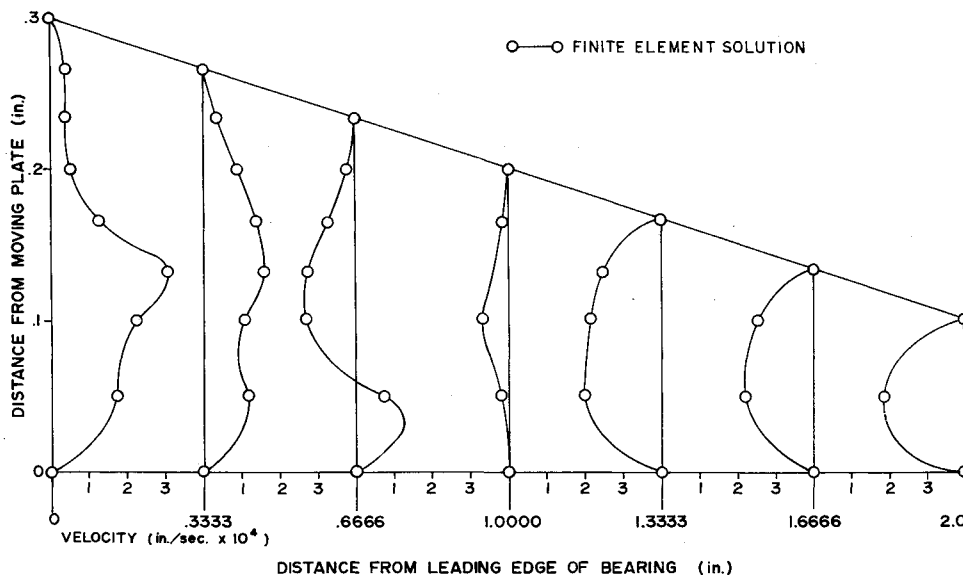


Fig. 7 y velocity component for the lubrication problem.

$$\begin{aligned}
 v_k &= (a_N + b_{Ni}x^i + c_{Nij}x^i x^j)v_k^N \\
 p &= (a_N + b_{Ni}x^i + c_{Nij}x^i x^j)p^N
 \end{aligned}
 \tag{50}$$

Here the six independent constants a_N, b_{Ni}, c_{Nij} ($c_{Nij} = c_{Nji}; i, j, k = 1, 2, 3; N = 1, 2, \dots, 6$) depend only on the local coordinates of the six nodes of the element. These local approximations determine all of the relevant arrays and matrices in the local momentum, energy, and continuity equations described earlier for each element.

Concerning convergence and accuracy of this particular approximation, we mention that Zlamal²⁴ has obtained the error estimate

$$|v - \bar{v}| \leq (K/\sin \theta)h^2
 \tag{51}$$

where v is a given continuously differentiable field, \bar{v} is a finite-element interpolant (i.e., \bar{v} coincides with v at the nodal points), h is the maximum diameter of all finite elements in a given mesh, θ is the smallest angle between any two sides of a triangle, and K is a constant independent of θ and h . Clearly, long flat elements lead to poorer conditioned systems than networks of isosceles triangles. In the case of elliptic and parabolic problems, estimates of the type in Eq. (51) lead directly to convergence and error estimates also involving $1/\sin \theta$ and, for energy convergence, Kh^4 . While the study of the stability and convergence of finite-element approximations of hyperbolic problems is scarcely beginning, preliminary results seem to indicate that the local character of the approximation lead to inherently better conditioned systems than conventional difference schemes of equal accuracy.

Couette Flow

The problem of unsteady Couette flow through the domain indicated in Fig. 1 is considered. The following boundary conditions were applied: 1) The x velocity component was assumed to be equal to 0.1 in./sec. and the y velocity component was assumed to be equal to zero at $y = 0.2$ in. 2) The x and y velocity components were prescribed as zero at $y = 0$. 3) The stress on the boundaries $x = 0$ and $x = 2.0$ in. was set equal to zero. 4) The gradient of the pressure in the direction perpendicular to the wall was zero at $y = 0$. As initial conditions, we set the pressure and the velocity vector equal to zero at all interior nodes at $t = 0$. The value of the mass density used was 0.00242 lbf.-sec.²/in.⁴ and the viscosity here and in all subsequent results was assumed to be 0.00362 lbf.-sec./in.²

In Fig. 2 the tangential velocity profile at $x = 0.5$ in. is presented at various times and shows good agreement with the exact solution.²¹ In Fig. 3, time histories of the tangential velocity

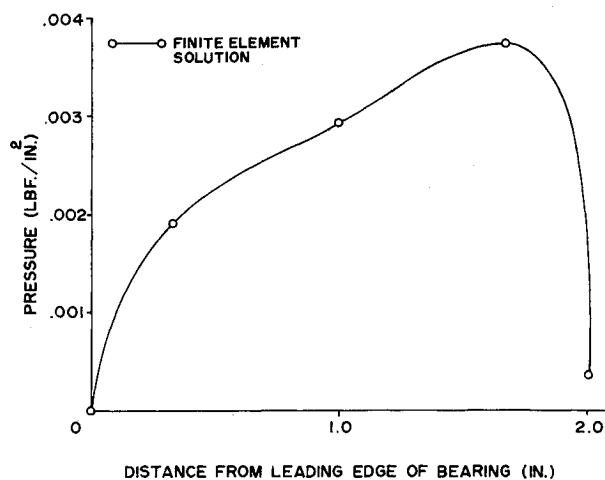


Fig. 8 Variation of pressure on the fixed slider bearing wall.

component at nodes 7, 8, and 9 are included. As can be seen, in the initial starting period negative tangential velocity components occur at several nodes. This was apparently due to either the applied stress boundary condition or the coarseness of the model used. Because of this constraint small transverse velocity components were computed. They were symmetric with respect to the lines connecting nodes 11 and 15 and 3 and 23. The time histories of the transverse velocity component at nodes 7 and 9 are given in Fig. 4.

An Incompressible Lubrication Problem

The two-dimensional flow of lubricant between a slide block or a slider bearing and a moving surface was determined. A fifteen element model, as illustrated in Fig. 5 was constructed. The following boundary conditions were applied: 1) The x -velocity component was 0.01 in./sec and the y velocity component was zero along $y = 0$. 2) The x and y velocity components were equated to zero along the slider bearing wall. 3) The stress at all unconstrained boundary nodes was prescribed as a hydrostatic pressure of 0.001 lbf./in.² 4) The gradient of the pressure perpendicular to the bearing wall was set equal to zero.

In the initial calculations, the convective inertial terms were ignored. The finite element solution for the velocity profile in the x direction is presented in Fig. 6. The transverse velocity profile is presented in Fig. 7, and the pressure along the inclined bearing

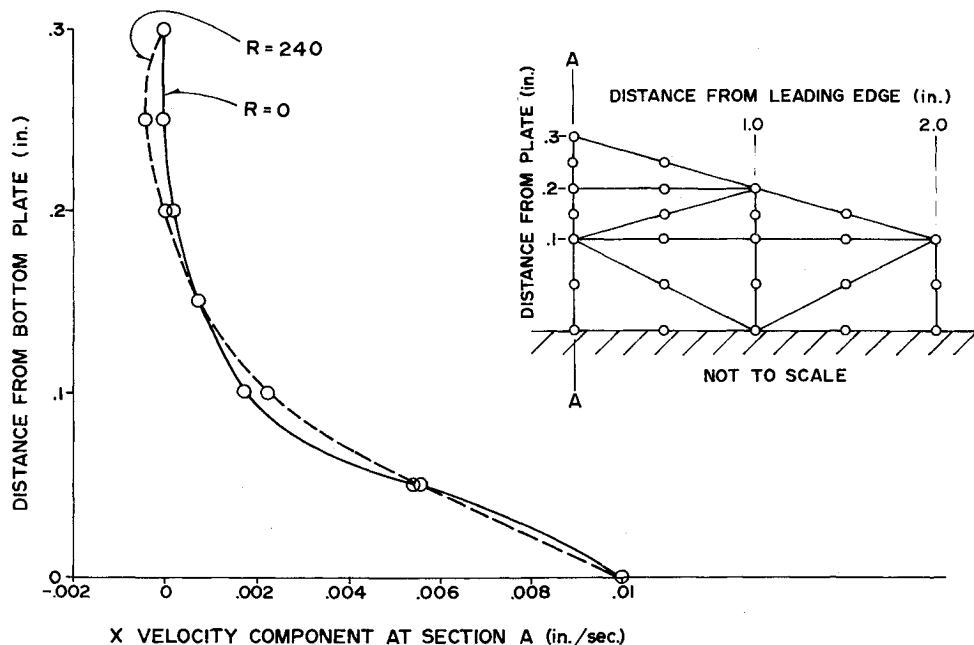


Fig. 9 x velocity component at section A as computed by the incremental densities technique.

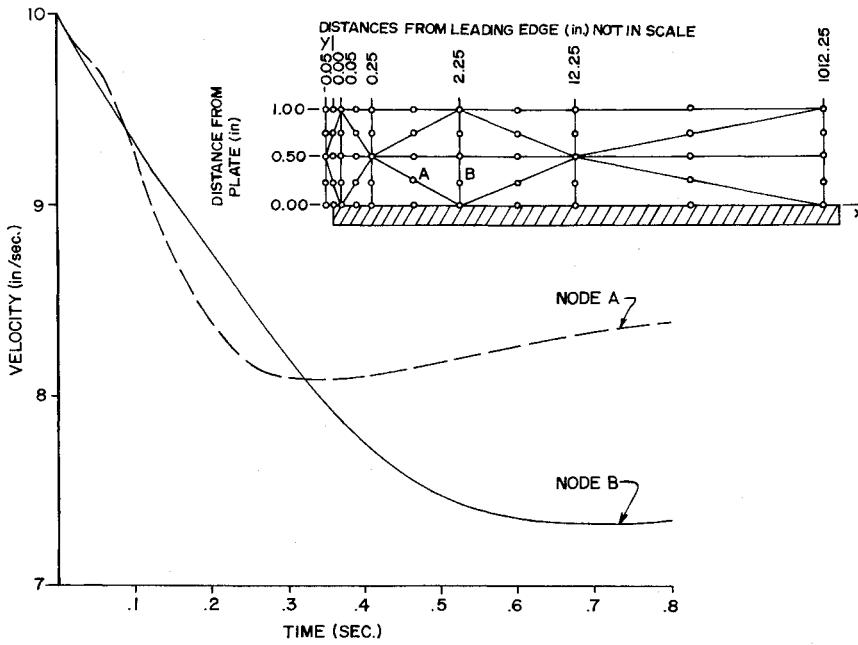


Fig. 10 Finite-element model of flow over a flat plate and time histories of the x velocity components at nodes A and B .

is indicated in Fig. 8. The transverse velocity profile changes direction between $x = 0.3333$ and $x = 0.6666$ in. resulting in a back flow in the bearing. The nonlinear convective terms were then included, and the bearing problem was solved by the incremental densities method described earlier. The resulting velocity profile in the x direction at a Reynolds number of 240 is included in Fig. 9. For Reynolds numbers larger than 240 more significant changes were observed in the velocity profile; these results are now being evaluated with a more detailed model.

Boundary-Layer Flow

The problem of transient boundary-layer formation over a flat plate was analyzed using the finite element grid of Fig. 10. This model is primarily useful for study of the velocity profile away from the leading edge of the plate. Thus results are presented for spatial points at least 1 in. from the leading edge where the model converges to the exact solution. In order to predict flow patterns at the leading edge, where high velocity gradients are encountered, a more detailed model of the flow would be required.

The following boundary conditions were specified: 1) The x velocity component was set equal to 10. in./sec. and the y velocity component was equated to zero at $x = -0.05$ in. 2) The x and y velocity components were zero at $y = 0$. 3) The gradient of the pressure in the direction normal to the wall was zero at $y = 0$. 4) The pressure was zero at all boundary nodes at which the velocity was not specified.

The initial conditions specified that the x velocity components

were 10. in./sec. and the y velocity components were zero at all unconstrained nodes at $t = 0$. The pressure was also zero at all nodes at time zero. A mass density of $1. \text{ lbf.} \cdot \text{sec.}^2 / \text{in.}^4$ was assumed.

Computed time histories of the x velocity components at nodes A and B are presented as representative variations in Fig. 10. In Fig. 11, the steady state finite-element solution is compared to the Blasius boundary-layer solution at specific points on the plate. Again, excellent agreement is obtained with a rather coarse mesh.

References

- ¹ Fix, G. and Larsen, K., "On the Convergence of SOR Iterations for Finite Element Approximations to Elliptic Boundary Value Problems," *SIAM Journal of Numerical Analysis*, Vol. 8, No. 3, 1970, pp. 536-547.
- ² Courant, R., "Variational Methods for the Solution of Problems of Equilibrium and Vibrations," *Bulletin, American Mathematical Society*, Vol. 49, Jan. 1943, pp. 1-23.
- ³ Turner, M. J., Clough, R. W., Martin, H. C., and Topp, L. P., "Stiffness and Deflection Analysis of Complex Structures," *Journal of the Aeronautical Sciences*, Vol. 23, No. 9, 1956, pp. 805-823.
- ⁴ Zienkiewicz, O. C., *The Finite Element Method in Engineering Science*, McGraw-Hill, London, 1972.
- ⁵ Zienkiewicz, O. C., Mayer, P., and Cheung, Y. K., "Solution of Anisotropic Seepage Problems by Finite Elements," *Proceedings of the American Society of Civil Engineers*, EM1, Vol. 92, 1966, pp. 111-120.
- ⁶ Martin, H. C., "Finite Element Analysis of Fluid Flows," AFFDL-

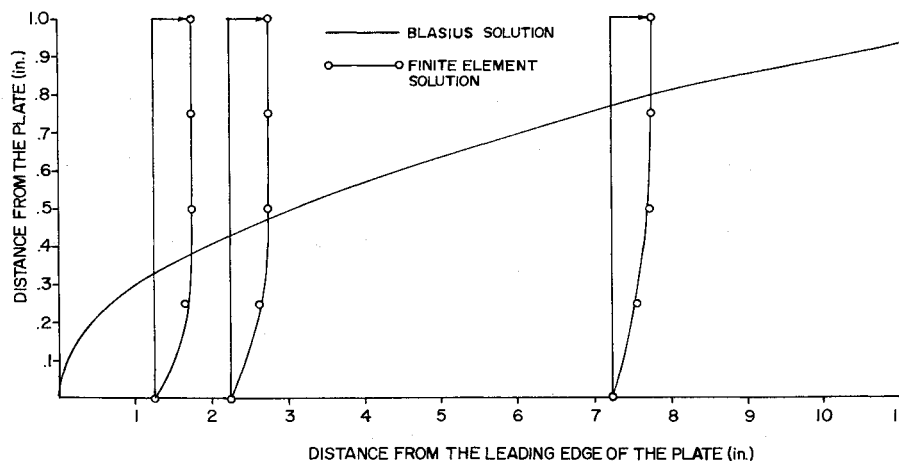


Fig. 11 Comparison of finite-element and Blasius solutions for the steady-state boundary layer on the front portion of the plate.

TR-68-150, Wright-Patterson Air Force Base, Ohio, 1969, pp. 517-535.

⁷ Oden, J. T., "A General Theory of Finite Elements; II Applications," *International Journal for Numerical Methods in Engineering*, Vol. 1, No. 3, 1969, pp. 247-259.

⁸ Oden, J. T. and Somogyi, D., "Finite-Element Applications in Fluid Dynamics," *Journal of the Engineering Mechanics Division*, ASCE, Vol. 95, No. EM4, 1969, pp. 821-826.

⁹ Oden, J. T., "Finite Element Formulation of Problems of Finite Deformation and Irreversible Thermodynamics of Nonlinear Continua," *Recent Advances in Matrix Methods of Structural Analysis and Design*, University of Alabama Press, Tuscaloosa, Ala., 1970.

¹⁰ Oden, J. T., "A Finite-Element Analogue of the Navier Stokes Equations," *Journal of the Engineering Mechanics Division*, ASCE, Vol. 96, No. EM4, 1970, pp. 529-534.

¹¹ Thompson, E. G., Mack, L. T., and Lin, F. S., "Finite-Element Method for Incompressible Slow Viscous Flow with a Free Surface," *Developments in Mechanics, Proceedings of the 11th Midwestern Mechanics Conference*, Iowa State University Press, Ames Iowa, Vol. 5, 1969, pp. 93-111.

¹² Tong, P., "The Finite Element Method in Fluid Flow Analysis," *Recent Advances in Matrix Methods of Structural Analysis and Design*, edited by R. H. Gallagher, Y. Yamada, and J. T. Oden, University of Alabama Press, Tuscaloosa, Ala., 1971, pp. 787-808.

¹³ Fujino, T., "Analysis of Hydrodynamic and Plate Structure Problems by the Finite Element Method," *Recent Advances in Matrix Methods of Structural Analysis and Design*, Edited by R. H. Gallagher, Y. Yamada, and J. T. Oden, University of Alabama Press, Tuscaloosa, Ala., 1971, pp. 725-786.

¹⁴ Argyris, J. H., "Two and Three-Dimensional Potential Flow by

the Method of Singularities," *The Aeronautical Journal of the Royal Aeronautical Society*, Vol. 73, Nov. 1969, pp. 959-961.

¹⁵ Argyris, J. H., Scharpf, D. W., "The Incompressible Lubrication Problem," *The Aeronautical Journal of the Royal Aeronautical Society*, Vol. 73, Dec. 1969, pp. 1044-1046.

¹⁶ Argyris, J. H., Mareczek, G., and Scharpf, D. W., "Two and Three-Dimensional Flow Using Finite Elements," *The Aeronautical Journal of the Royal Aeronautical Society*, Vol. 73, Nov. 1969, pp. 961-964.

¹⁷ Reddi, M. M., "Finite-Element Solution of the Incompressible Lubrication Problem," *Transactions of the ASME, Journal of Lubrication*, Vol. 91, July 1969, pp. 524-533.

¹⁸ Baker, A. J., "A Numerical Solution Technique for Two-Dimensional Problems in Fluid Dynamics Formulated with the Use of Discrete Elements," TN-TCTN1005, Bell Aerosystems Co., Niagara Falls, N.Y., 1970.

¹⁹ Herting, D. N., Joseph, J. A., Kuusinen, L. R., and MacNeal, R. H., "Acoustic Analysis of Solid Rocket Motor Cavities by a Finite Element Method," *NASTRAN: User's Experience*, Vol. I, NASA TMX-2378, 1971.

²⁰ Oden, J. T., *Finite Elements of Nonlinear Continua*, McGraw-Hill, New York, 1971.

²¹ Schlichting, H., *Boundary-Layer Theory*, McGraw-Hill, New York, 1968.

²² Eringen, A. C., *Mechanics of Continua*, Wiley, New York, 1967.

²³ Ladyzhenskaya, O. A., *The Mathematical Theory of Viscous Incompressible Flow*, Gordon and Breach, New York, 1969.

²⁴ Zlamal, M., "On the Finite Element Method," *Numerische Mathematik*, Vol. 12, 1968, pp. 394-409.